Methane Steam Reforming by Microporous Catalytic Membrane Reactors

Toshinori Tsuru, Koji Yamaguchi, Tomohisa Yoshioka, and Masashi Asaeda
Dept. of Chemical Engineering, Hiroshima University, Higashi-Hiroshima 739-8527, Japan

DOI 10.1002/aic.10215
Published online in Wiley InterScience (www.interscience.wiley.com).

Methane steam reforming, with and without added oxygen, was theoretically and experimentally investigated using microporous silica membranes, thus allowing the permeation of hydrogen as well as other gases in reactants and products. A simulation of catalytic membrane reactors was carried out for a cocurrent, isothermal, and plug-flow–type membrane reactor with the selective permeation of hydrogen through microporous membranes. The effect of operating conditions on the conversion of methane and hydrogen production is discussed with the aid of two dimensionless numbers, the Damköhler number (Da) and the permeation number (θ). Methane conversion, X_{CH4}, has approximately the same dependency on permeation number in terms of the permeability ratios of hydrogen over nitrogen, whereas the purity of hydrogen in the permeate increased with increasing hydrogen selectivity. Catalytic membrane reactors, consisting of a silica microporous layer and a Ni-catalyst layer, were prepared. The permeability ratio of hydrogen over steam, $\alpha(H_2/H_2O)$, which ranged from 1 to 20, showed a relatively good correlation with that for helium over hydrogen, $\alpha(He/H_2)$. Catalytic membrane reactors showing a hydrogen selectivity over nitrogen of 30–100, with hydrogen permeances of 0.5–3 $\times$ 10^{-7} mol m^{-2} s^{-1} Pa^{-1}, were applied to the steam reforming of methane with and without the addition of oxygen. The reaction was carried out at 500°C, and the feed and permeate pressure were maintained at 100 and 20 kPa, respectively. Methane conversion, X_{CH4}, increased up to approximately 0.8 beyond the equilibrium conversion of 0.44 by extracting hydrogen in permeate stream. © 2004 American Institute of Chemical Engineers *AIChE J,* 50: 2794–2805, 2004

Keywords: catalytic membrane reactor, methane steam reforming, autothermal, porous silica membranes, hydrogen, simulation

Introduction

Hydrogen is a clean fuel that does not generate carbon dioxide and has attracted a great deal of attention for use as a fuel gas in polymer electrolyte fuel cells. Technology for the production and purification of hydrogen represents key factors, if hydrogen is to be used in future energy systems. Hydrogen can be produced by the steam reforming of methane, and conventionally purified by distillation and pressure-swing adsorption (PSA). Membrane separation is a recently developed technology for hydrogen purification.

Membrane reactors, in which reaction and separation occur in one unit, have attracted considerable attention, especially for hydrogen production by the steam reforming of methane. This area has become even more attractive with the development of inorganic membranes that support high-temperature applications (Sanchez and Tsotsis, 2002). The conversion of methane is limited because the main reaction of methane reforming, that is, the steam reforming of methane (SRM), $CH_4+H_2O = CO + 3H_2$, and the water-gas shift reaction, $CO + H_2O = CO_2 +$

Correspondence concerning this article should be addressed to T. Tsuru at tsuru@hiroshima-u.ac.jp.

H_2, are subject to thermodynamic equilibrium. The steam reforming reaction, which is endothermic and therefore favored at high temperature, is conventionally operated at approximately 800°C. Membrane reactors would be expected to reduce the operating temperature by shifting the SRM by the use of hydrogen permselective membranes. A number of studies of membrane reactors for methane steam reforming using dense membranes such as palladium (Sanchez and Tsotsis, 2002; Uemiya et al., 1991) have been reported. In terms of palladium membranes, which allow 100% pure hydrogen in the permeate stream, several disadvantages such as high cost and degradation by acidic gases and carbon have been indicated (Hsieh, 1996; Sanchez and Tsotsis, 2002). On the other hand, a limited number of papers have reported on membrane reactors for methane reforming that use porous membranes: steam reforming of methane using alumina membranes (Chai et al., 1994; Tsotsis et al., 1993) and silica membranes (Tsuru et al., 2001; Yoshida et al., 2001a), and CO_2 reforming of methane using microporous silica membranes (Prabhu et al., 2000a,b). Membrane characteristics such as the permeability of water vapor, a crucial factor that influences the performance of membrane reactors, have not been extensively investigated. Additional experimental investigations of membrane reactors using porous membranes would be important from the viewpoint of the dependency of the performance of membrane reactors on operating conditions (flow rate, pressure).

Simulation studies of membrane reactors often assume the use of palladium membranes as hydrogen semipermeable membranes, and the performance (such as temperature profile along the axial direction) is discussed in detail (Kim et al., 1999). On the other hand, porous membranes, which also show the conversion larger than the equilibrium as membrane reactors, have not been extensively discussed (Oklany et al., 1998; Prabhu et al., 2000b). Porous membranes, the separation mechanism of which is based on molecular sieving, permit the permeation of hydrogen as well as other gases, resulting in a reduced hydrogen yield and permeate concentration (Hwang and Onuki, 2001; Itoh, 1983; Yogeshwar et al., 1995). In other words, the performance of membrane reactors for methane reforming depends on the characteristics of the membrane used (selectivity, permeability) and reaction conditions (feed flow rate, reaction rate, pressure), and an understanding of these effects on the performance of the membrane reactors constitutes an important issue.

In this study, methane reforming was simulated using a one-dimensional (1-D) isothermal plug-flow model under cocurrent flow conditions. The performance of the membrane reactor in terms of methane conversion and hydrogen yield, are discussed based on membrane selectivity (α); the Damköhler number (Da), which corresponds to the ratio of reaction rate to feed flow rate; and the permeation number (θ), which is the ratio of permeate to feed flow rate. Moreover, catalytic membrane reactors, consisting of a silica hydrogen separation layer on Ni-catalyst impregnated substrates, were prepared and used for methane steam reforming with the addition of oxygen.

Simulation of Membrane Reactors of Methane Reforming

The reactions discussed in the present study are the steam reforming of methane (SRM) and the SRM reaction with added oxygen, which will be abbreviated as the oxygen-added steam reforming reaction of methane (OSR) in later sections. According to Xu and Froment (1989) and Adris et al. (1991), the following reactions can be assumed for the steam reforming of methane

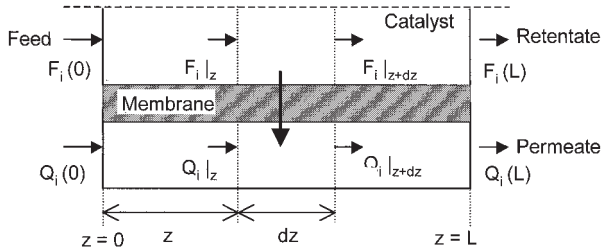

Figure 1. Membrane reactor.

F_i and Q_i are the molar flow rate into the feed and permeate streams, respectively.

$$CH_4 + H_2O = CO + 3H_2 \qquad \Delta H_{298} = 206 \text{ kJ/mol} \quad (1)$$

$$CO + H_2O = CO_2 + H_2 \qquad \Delta H_{298} = -41 \text{ kJ/mol} \quad (2)$$

$$CH_4 + 2H_2O = CO_2 + 4H_2 \qquad \Delta H_{298} = 165 \text{ kJ/mol} \quad (3)$$

For the case of oxygen addition, the oxidation of methane is assumed as follows

$$CH_4 + 0.5O_2 \rightarrow CO + 2H_2 \qquad \Delta H_{298} = -36 \text{ kJ/mol} \quad (4)$$

$$CH_4 + 2O_2 \rightarrow CO_2 + 2H_2O \qquad \Delta H_{298} = -803 \text{ kJ/mol} \quad (5)$$

SRMs 1 and 3 are endothermic, whereas reactions 4 and 5 are exothermic. The possibility of an autothermal reaction, that is, a self-sustaining reaction in terms of reaction heat, was indicated for the case of the SRM reaction with added oxygen (OSR) in a palladium membrane reactor (Chen et al., 2003; Grace et al., 2001).

Figure 1 shows the schematic reaction model used for the simulation of a membrane reactor. The following assumptions were made: (1) plug flow in the feed and permeate stream; (2) an isothermal reaction, which occurs on the catalysts in the feed stream, at 500°C; and (3) negligible pressure drop along the axial direction. Table 1 summarizes the rate equations and rate factors for reactions 1–3 (Adris et al., 1991; Xu and Froment, 1989). The oxidation of methane was assumed to be completed at the inlet of the membrane reactor based on reaction 5, which produces CO_2 and H_2O, followed by reactions 1–3.

The molar flow rate in the feed and permeate streams, F_i and Q_i, can be described as follows in a plug flow reactor (Tsotsis et al., 1993).

Feed Stream (Retentate Flow)

$$\frac{dF_i}{dz} = \sum_{j=1,2,3} \nu_{i,j} R_j w_{cat} - sP_i(x_i p_h - y_i p_l) \quad (6)$$

Table 1. Kinetic Rate and Parameters of Methane Reforming

$CH_4 + H_2O = CO + 3H_2$	$R_1 = k_1\{(p_{CH_4}p_{H_2O}/p_{H_2}^{2.5}) - (p_{H_2}^{0.5}p_{CO}/K_{1e})\}/DEN^2$
$CO + H_2O = CO_2 + H_2$	$R_2 = k_2\{(p_{CO}p_{H_2O}/p_{H_2}) - (p_{CO_2}/K_{2e})\}/DEN^2$
$CH_4 + 2H_2O = CO_2 + 4H_2$	$R_3 = k_3\{(p_{CH_4}p_{H_2O}^2/p_{H_2}^{3.5}) - [p_{H_2}^{0.5}p_{CO_2}/(K_{1e}K_{2e})]\}/DEN^2$
where $DEN = 1 + K_{CO}p_{CO} + K_{H_2}p_{H_2} + K_{CH_4}p_{CH_4} + K_{H_2O}p_{H_2O}/p_{H_2}$	

Rate factors $k_j = A_j\exp(-\Delta E_j/RT)$		
k_1 [mol $Pa^{0.5}$/(kg-cat s)]	$A_1 = 3.71 \times 10^{17}$	$\Delta E_1 = 240.1$ kJ/mol
k_2 [mol/(kg-cat s $Pa^{0.5}$)]	$A_2 = 5.43$	$\Delta E_2 = 67.13$ kJ/mol
k_3 [mol $Pa^{0.5}$/(kg-cat s)]	$A_3 = 8.96 \times 10^{16}$	$\Delta E_3 = 243.9$ kJ/mol
Equilibrium constant		
K_{1e} [Pa^2] $= 1.03 \times 10^{10}\exp[30.4197 - (27106.2/T)]$		
K_{2e}[—] $= \exp[-3.79762 + (4159.54/T)]$		
Adsorption parameters $K_i = B_i\exp(-\Delta H_i/RT)$		
K_{CH_4} [Pa^{-1}]	$B_{CH_4} = 6.65 \times 10^{-9}$	$\Delta H_{CH_4} = -38.28$ kJ/mol
K_{H_2O} [—]	$B_{H_2O} = 1.77 \times 10^5$	$\Delta H_{H_2O} = 88.68$ kJ/mol
K_{CO} [Pa^{-1}]	$B_{CO} = 8.23 \times 10^{-10}$	$\Delta H_{CO} = -70.65$ kJ/mol
K_{H_2} [Pa^{-1}]	$B_{H_2} = 6.12 \times 10^{-14}$	$\Delta H_{H_2} = -82.9$ kJ/mol

Permeate Stream

$$\frac{dQ_i}{dz} = sP_i(x_i p_h - y_i p_l) \tag{7}$$

where R_j and $\nu_{i,j}$ are the reaction rate and stoichiometric number of the jth reforming reaction ($j = 1, 2, 3$), respectively, as shown in Table 1. P_i is the permeance of the ith component; p_h, p_l, x_i, and y_i are the total pressure of feed and permeate, and the mole fraction of the ith component in the feed and permeate, respectively. w_{cat} and s indicate the catalyst weight and membrane area per membrane unit length.

Equations 6 and 7 can be converted into dimensionless equations, using dimensionless numbers, as shown in Table 2

$$\frac{df_i}{d\zeta} = \sum_i \mathrm{Da}\ \nu_{i,j}R_j^* - \frac{\theta(x_i - y_i p_r)}{\alpha_i} \tag{8}$$

$$\frac{dq_i}{d\zeta} = \frac{\theta(x_i - y_i p_r)}{\alpha_i} \tag{9}$$

The dimensionless reaction rate R_j^* was normalized with $R_1^{\max}$, defined as the forward rate of reaction 1 based on the inlet composition. According to Mohan and Govind (1986, 1988) and Yogeshwar et al. (1995), the performance of a membrane reactor can be evaluated using the Damköhler number Da and the permeation number θ. The Damköhler number indicates the ratio of the maximum reaction rate to the inlet flow rate of methane, and can be interpreted as a measure of residence time in reactor and space velocity. Infinite Da can be achieved when the smallest feed flow rate or the largest loading of catalysts is used, and shows the equilibrium composition at any axial location. The permeation number θ, defined as the ratio of the maximal hydrogen permeate flow rate to the feed flow rate of methane, serves as a measure of the effect of the extraction of hydrogen.

Hydrogen permeance P_{H_2}, the permeability ratio of hydrogen over nitrogen $\alpha(H_2/N_2)$, and that of hydrogen to steam $\alpha(H_2/H_2O)$ were used as parameters of membrane performance for the simulation. Gaseous molecules such as N_2, CH_4, CO, and CO_2, which have relatively large molecular sizes, were assumed to permeate through pinholes left in the hydrogen semipermeable porous membranes, based on Knudsen diffusion (Yoshioka et al., 2001). Therefore, the permeances of CH_4, CO, and CO_2 were assumed to show a Knudsen selectivity to nitrogen permeance, as shown in Table 3. The selectivity of hydrogen to steam was reported to be dependent on the conditions used to prepare the membranes (Sea et al., 1998); it has been reported that amorphous silica prepared by the sol–gel method showed $\alpha(H_2/N_2)$ and $\alpha(H_2/H_2O)$ values of 450 and 3, respectively (Tsuru et al., 2001). Membrane permeation performance is also dependent on the pressure of the feed and permeate streams, and can be normalized using the pressure ratio p_r, defined as the ratio of permeate pressure to feed pressure.

The simulation was carried out at a temperature of 500°C, a feed pressure (p_h) of 100 kPa, and a pressure ratio (p_r) of 0.2, as summarized in Table 3. The ratio of feed flow rate of steam to methane, S/C ($=F_{H_2O}/F_{CH_4}$), was fixed at 3, whereas that of oxygen to methane, O/C ($=F_{O_2}/F_{CH_4}$), was varied from 0 to 0.4. Based on Kim et al. (1999), the inlet flow rate of hydrogen can be assumed to be 10^{-4} relative to methane, which is necessary for the calculation for reactions 1–3. The performance of a membrane reactor was compared based on methane conversion (X_{CH4}) and permeate hydrogen yield (Y_{H2}).

Experimental

Hydrogen-semipermeable catalytic membranes

A 40 wt % nickel nitrate solution was used in the preparation of the catalytic membranes. The nickel catalyst was impregnated by immersing an α-alumina porous substrate (pore size 1 μm, outer diameter 10 mm, inner diameter 8 mm, length 9 cm) in the nickel nitrate solution, followed by drying at room temperature more than 12 h and firing at 500°C in air. The hydrogen separation layer was then formed on the outer surface of the substrates. Catalytic membranes were fired in air at 500°C, and reduced to the elemental state by treatment with hydrogen at 500°C before use (Tsuru et al., 2001).

The hydrogen separation layer was prepared by a sol–gel process using silica sol solutions. Colloidal silica sol solutions were prepared by hydrolysis reaction of 2.5–10 g of tetraethoxysilane (TEOS) with 100 g of water using 0.5 cm^3 of nitric acid as a catalyst for 1 h, followed by condensation reaction at the boiling point for 12 h after adding 500 g of water and 1.5 cm^3 of nitric acid. Several sol solutions, having different colloidal

Table 2. Dimensionless Parameters Used in the Simulation of the Membrane Reactor

Permeation number: $\theta = \dfrac{P_{H_2}sLp_h}{F_{CH_4,0}}$
Damköhler number: $\mathrm{Da} = \dfrac{R_1^{\max}W_{cat}}{F_{CH_4,0}}$ (where $R_1^{\max} = k_1(p_{CH_4}p_{H_2O}/p_{H_2}^{2.5})/DEN^2$)
Axial position: $\zeta = z/L$; dimensionless reaction rate: $R_j^* = R_j/R_1^{\max}$

Table 3. Membrane Performance and Operating Conditions Used for Simulation

Membrane performance	$P_{CH_4} = P_{H_2}/\alpha(H_2/N_2) \times 1.323$	$P_{H_2O} = P_{H_2}/\alpha(H_2/H_2O)$
	$P_{CO} = P_{H_2}/\alpha(H_2/N_2) \times 1.0$	$P_{CO_2} = P_{H_2}/\alpha(H_2/N_2) \times 0.798$
Operating condition	$p_r\ (=p_l/p_h) = 0.2\ (p_h = 100$ kPa)	500°C, isothermal
	S/C $(=F_{H_2O}/F_{CH_4}) = 3$	O/C $(=F_{O_2}/F_{CH_4}) = 0$–0.4

diameters, were prepared by controlling TEOS concentration in the condensation reaction. The Ni-impregnated α-alumina porous substrates were first deposited using α-alumina particles (average diameter 180 nm; Sumitomo Chemical Co., Tokyo, Japan) mixed with a colloidal sol solution, followed by coating with sol solutions of larger to smaller colloidal diameters. Details of this procedure are described elsewhere (Asaeda and Yamasaki, 2001; Tsuru et al., 1998, 2001; Yoshida et al., 2001b,c; Yoshioka et al., 2001).

Membrane reaction for methane reforming

Gas permeances of pure gases (He, H_2, N_2, CO_2,) were measured using a catalytic membrane reactor system, as shown in Figure 2. The pressure of the feed stream, p_h, was maintained at 200 kPa, whereas that of the permeate stream, p_l, was maintained at atmospheric pressure. Before use for the membrane reaction, porous silica membranes were hydrothermally treated at 500°C for several hours at atmospheric pressure, using a mixed feed of hydrogen and steam (mole fraction 0.5/0.5) and a nitrogen sweep in the permeate stream, and permeances of H_2, N_2, and H_2O were simultaneously calculated. The temperature of the outside of the catalytic membrane housing was controlled at 500°C, and the temperature inside the catalytic membrane was measured using a movable thermocouple set inside the tubular membrane.

A mixture of methane and steam (S/C = 3) was continuously supplied to the catalytic membranes at a methane flow rate of approximately 0.5–20 $\times$ 10^{-6} mol s^{-1}. The feed stream was approximately atmospheric, whereas the permeate stream was evacuated down to approximately 20 kPa using a diaphragm pump. The reaction was carried out at 500°C. Reactant gaseous mixtures were fed to the inner stream of the cylindrical membranes.

Gas compositions were determined using two types of online gas chromatographs: GC-1 and GC-2. GC-1, equipped with a packed column of Gaschropack 54 at an operating temperature of 180°C, was used for the analysis of water vapor and CO_2, whereas GC-2, with molecular sieves operated at 80°C, was used for the analysis of other gases such as H_2, O_2, N_2, CH_4, and CO after removing water vapor by cold traps. First, partial pressures of H_2O and CO_2 were determined based on GC-1 analysis, and then the total pressure of other gases including H_2, O_2, N_2, CH_4, and CO, the mole fractions of which were determined by GC-2 analysis, was calculated; the mole fractions of each component in retentate and permeate streams could be determined by using two gas chromatographs. Therefore, based on the flow rates measured with soap film meters, assumed to consist of noncondensable gas (H_2, O_2, N_2, CH_4, CO, and CO_2), the permeate and retentate flow rates of each component were determined. The material balance of carbon, hydrogen, and oxygen atoms was within the maximum error of less than 10%.

Results and Discussion

Simulation study on membrane reactor

Figure 3 shows the flow rates of components in the feed-side (retentate) and permeate stream along the axis for the case of a permeability ratio of hydrogen over nitrogen, $\alpha(H_2/N_2)$, of 100, and a permeation number θ of 10. Feed-side CH_4 flow rate for the case of Da = 100, which is shown in Figure 3a as the normalized flow rate with the inlet flow rate of methane,

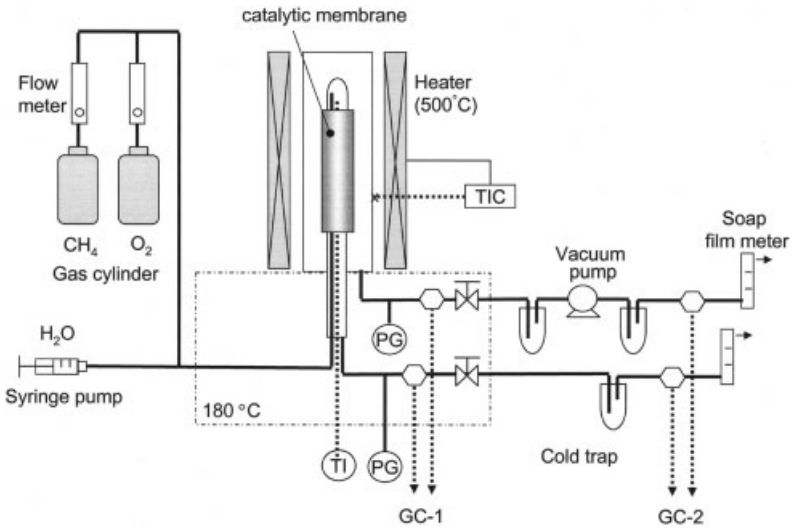

Figure 2. Experimental apparatus of a membrane reactor system.

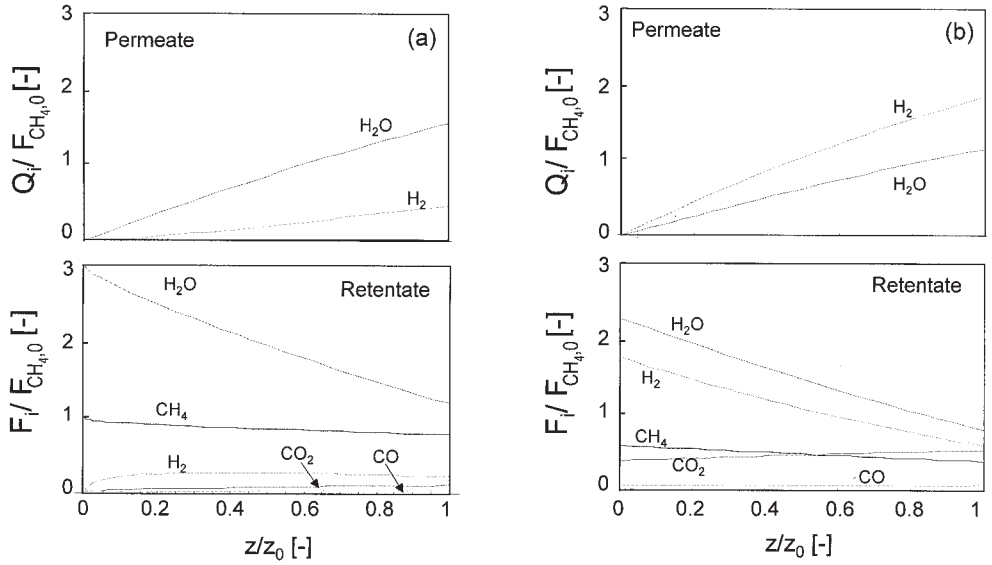

Figure 3. Flow rate normalized with CH_4 feed flow rate along the axis.

(a) Da = 100; p_h = 100 kPa, p_r = 0.2; S/C = 3; $\alpha(H_2/N_2)$ = 100, $\alpha(H_2/H_2O)$ = 3; θ = 10. (b) Da = ∞; p_h = 100 kPa, p_r = 0.2; S/C = 3; $\alpha(H_2/N_2)$ = 100, $\alpha(H_2/H_2O)$ = 3; θ = 10.

deceases gradually because of the steam reforming reaction along the axis. On the other hand, steam in the retentate stream is consumed by reaction with methane and permeates the membrane because of its relatively large permeability and, consequently, the normalized flow rate of steam deceases drastically from a value of 3 at the inlet to an approximate value of 1 at the outlet. Figure 3b shows the case of infinite Da number; feed-side composition, which satisfies the equilibrium of the reactions 1–3 at any axial location, changes as a result of selective permeation through the microporous membrane. It is clear that a larger hydrogen yield can be achieved when the Da number is larger.

The effect of the Damköhler number (Da) and the permeation number (θ) on methane conversion, X_{CH4}, is shown in Figure 4. X_{CH4} decreases with a decrease in Da, which corresponds to a small catalyst loading and a large inlet flow rate. The infinite Da number, which allows a local equilibrium in the feed-side composition, as a result of the infinite high reaction rate compared with the feed flow rate of methane, shows the largest conversion. The conversion at infinite Da and $\theta = 1$ is in good agreement with the equilibrium conversion (X_{CH4} = 0.44) for S/C, the ratio of feed flow rate of steam to methane of 3, and a reaction pressure of 100 kPa. Small values of θ indicate a small effect of selective permeation on methane conversion, and conversions at $\theta = 1$ show approximately good agreement with those achieved without membrane permeation. An increase in permeation number θ, which can be achieved either by large hydrogen permeability and membrane area or by decreasing the feed flow rate of methane, causes a significant effect on the enhancement of methane conversion and, consequently, methane conversion increases up to 0.7 beyond the equilibrium conversion of 0.44. It should be noted that X_{CH4} at any value of Da increases with an increase in θ.

Hydrogen yield Y_{H2}, which is defined as the ratio of permeated hydrogen molar flow rate to inlet methane flow rate, increases with an increase in θ and Da. It should be noted that the maximal

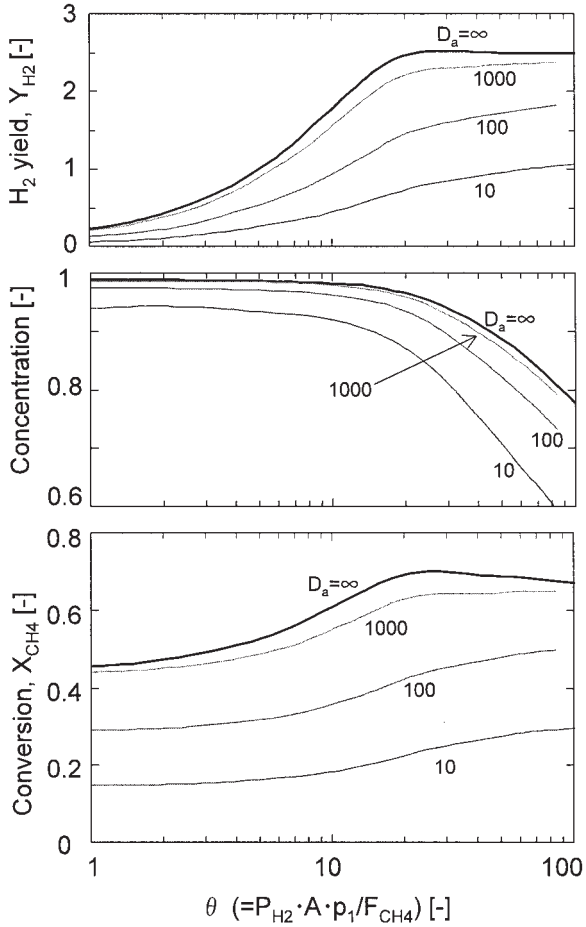

Figure 4. Effect of Damköhler number (Da) on permeate hydrogen yield (Y_{H2}), H_2 concentration in permeate, and CH_4 conversion (X_{CH4}) as a function of permeation number.

SRM; p_h = 100 kPa, p_r = 0.2; S/C = 3; $\alpha(H_2/N_2)$ = 100, $\alpha(H_2/H_2O)$ = 3.

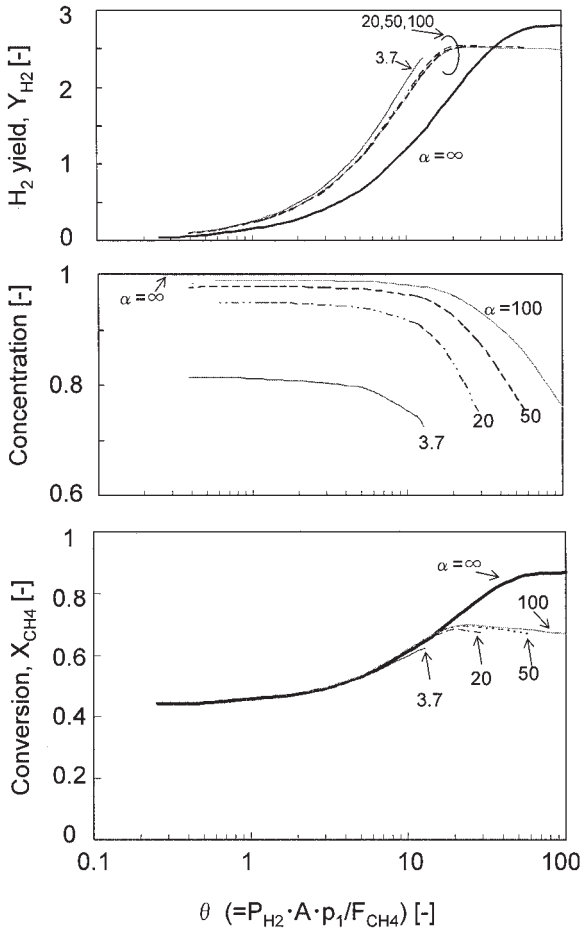

Figure 5. Effect of selectivity of $\alpha(H_2/N_2)$ on permeate hydrogen yield (Y_{H2}), H_2 concentration in permeate, and CH_4 conversion (X_{CH4}) as a function of permeation number.

SRM; Da = ∞, p_h = 100 kPa, p_r = 0.2; S/C = 3; $\alpha(H_2/H_2O)$ = 3.

Y_{H2} is 4 for the case of the complete recovery of hydrogen in the permeate stream and 100% methane conversion. Hydrogen concentration in the permeate, defined as mole fraction based on dry gas, shows a tendency to decrease with an increase in θ and with a decease in Da. This is because large θ and small Da allow the permeation of product gas (CO, CO_2) and reactant gases (CH_4, H_2O), respectively. The effect of θ on conversion appears to show a similar tendency for any Da number and, therefore, the case of infinite Da will be discussed below.

Figure 5 shows the effect of θ and $\alpha(H_2/N_2)$ on X_{CH4}, Y_{H2}, and hydrogen concentration. For the comparison, the calculated results for a palladium membrane ($\alpha = \infty$) and Knudsen-selective membranes ($\alpha = 3.7$) are also included in the figure. Methane conversion increases with an increase in θ and shows almost the same dependency, irrespective of $\alpha(H_2/N_2)$, because the enhancement in methane conversion is highly dependent on the permeation of hydrogen. However, the maximal conversion of methane for porous membranes is approximately 0.7 because of the leakage of reactants (CH_4 and H_2O). Hydrogen concentration in the permeate increases with an increase in $\alpha(H_2/N_2)$, reaching 100% for a palladium membrane ($\alpha = \infty$). On the other hand, porous membranes show larger Y_{H2} values than the palladium membrane for the case where θ is lower than 30. As is clear from Figure 3, porous membranes allow the permeation of steam, present as the major component in the retentate stream, which decreases the partial pressure of hydrogen in the permeate, resulting in an increase in hydrogen permeation, compared with a palladium membrane. It should be noted that simulated curves of porous membranes show upper limits in terms of θ because the retentate flow rate decreases with θ and diminishes at a certain value, that is, maximal θ. Another tendency to be identified is that X_{CH4} shows a maximum as a function of θ because of the contribution of reverse reaction of steam reforming of methane. At large θ, partial pressure of H_2O in the feed stream decreases drastically because of reaction with methane as well as membrane permeation, whereas CO and CO_2, having much lower permeance than that of H_2O, show increased partial pressure, as can be speculated from Figure 3, resulting in enhancement of reverse reaction of steam reforming of methane.

Figure 6 shows the effect of the permeability ratio of hydrogen to water vapor, $\alpha(H_2/H_2O)$. As will be discussed below,

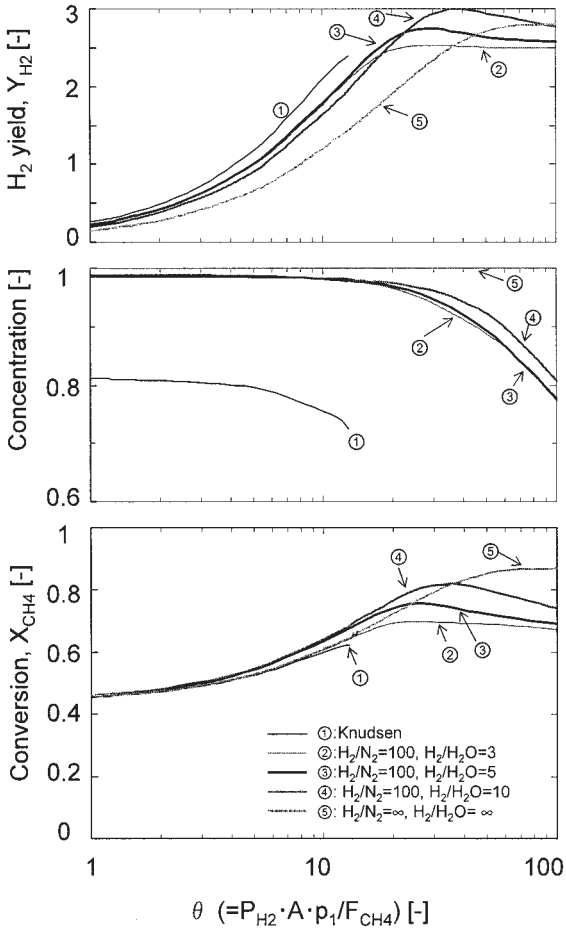

Figure 6. Effect of selectivity of H_2/H_2O on permeate hydrogen yield (Y_{H2}), H_2 concentration in permeate, and CH_4 conversion (X_{CH4}) as a function of permeation number.

SRM; Da = ∞, p_h = 100 kPa, p_r = 0.2; S/C = 3; $\alpha(H_2/N_2)$ = 100.

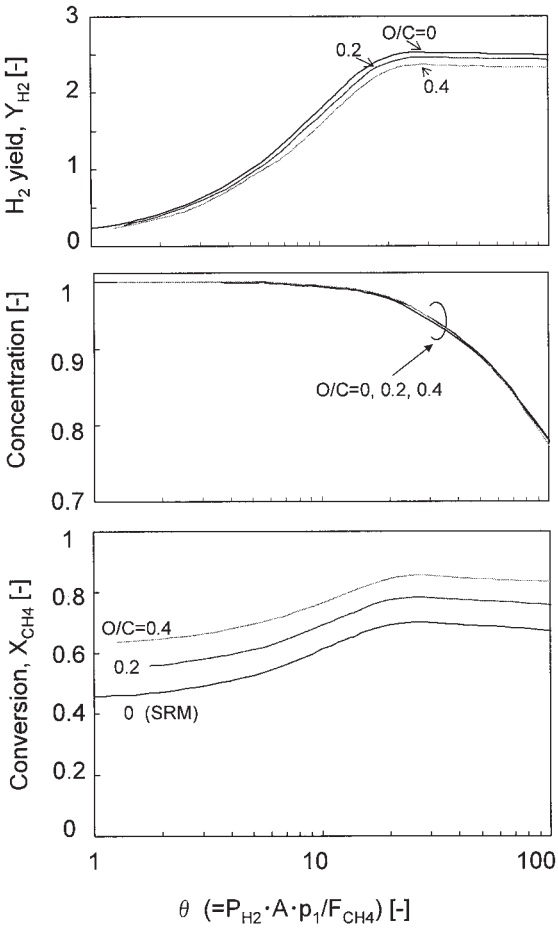

Figure 7. Effect of O/C on permeate hydrogen yield (Y_{H2}), H_2 concentration in permeate, and CH_4 conversion (X_{CH4}) as a function of permeation number.

OSR; Da = ∞, p_h = 100 kPa, p_r = 0.2; S/C = 3; $\alpha(H_2/N_2)$ = 100, $\alpha(H_2/H_2O)$ = 3.

porous silica membranes show $\alpha(H_2/H_2O)$ values ranging from approximately 2 to 15. With an increase in $\alpha(H_2/H_2O)$, hydrogen yield, hydrogen concentration, and methane conversion increase, which increases the performance of the membrane reactor. This is because larger $\alpha(H_2/H_2O)$ values reduce the leakage of steam into the permeate. By comparing Figures 5 and 6, it can be concluded that a small enhancement in the selectivity of hydrogen over steam is quite effective for improving the performance of the membrane reactor.

Autothermal reforming reactions, which can be realized by adding oxygen to the feed flow in the steam reforming of methane, are attractive because the combustion of methane could provide the heat required for the endothermic reaction of steam reforming. Figure 7 shows the effect of oxygen addition for the case of a constant S/C of 3 in the feed. The addition of oxygen increases methane conversion and only slightly decreases hydrogen yield, whereas hydrogen in the permeate is present at approximately the same concentration.

As discussed above, dimensionless numbers, permeation number θ and Damköhler number Da, are quite useful parameters in understanding the dependency of the performance of membrane reactors on operating conditions (feed flow rate, reaction rate determined by types of catalyst and the amount in membrane reactor) and membrane performance (hydrogen permeance, permeability ratio to other gases).

Catalytic membranes

Figure 8 shows a cross section of a catalytic membrane. An intermediate layer can be observed on the outer surface of the substrate with a thickness of approximately 1–2 μm. The top layer, which functions for hydrogen permselectivity, was prepared by coating colloidal sol solutions and the thickness appears to be less than 1 μm. Nickel catalysts of approximately 0.1 μm in particle size were observed on the α-alumina particles of several micrometers, which consisted of the α-alumina support. The average amount of Ni impregnation was approximately 0.25 g (as NiO) by weighing α-alumina supports before and after Ni impregnation. Several types of membrane reactor configurations have been proposed: packed-bed membrane reactors (PBMR), fluidized-bed membrane reactors (FBMR), and catalytic membrane reactors (CMR). PBMR and FBMR consist of permselective membranes and catalysts either in a packed or fluidized bed. Catalytic membranes, which have the functions of both catalysis and separation in one membrane, can be applied in a more compact manner than can other types of membrane reactors and have been recently applied to methane reforming (Kurungot et al., 2003; Tsuru et al., 2001).

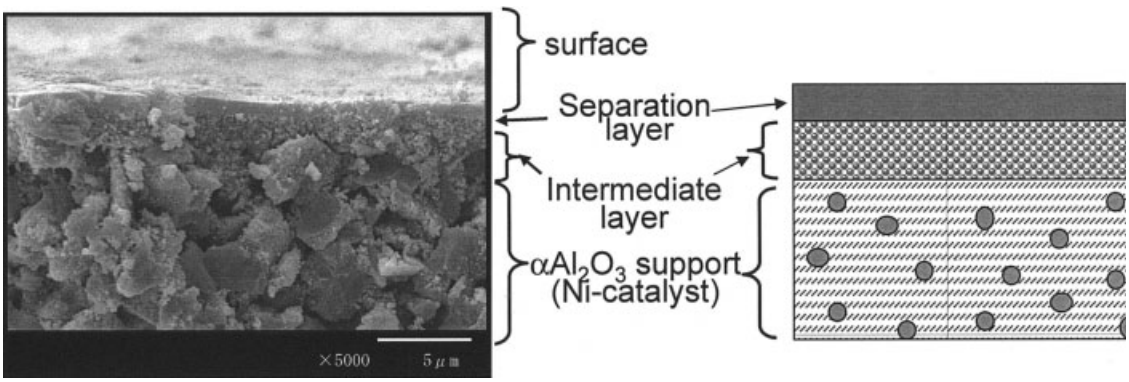

Figure 8. Cross section of a catalytic membrane.

Ni catalysts were impregnated inside an α-Al_2O_3 porous substrate.

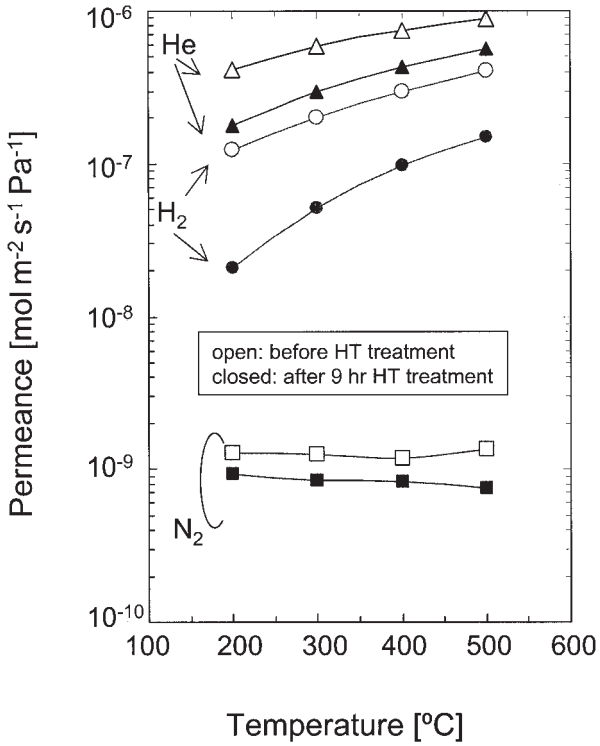

Figure 9. Permeances of He, H_2, and N_2 before and after hydrothermal treatment.

Hydrothermal treatment (HT) was carried out at 50 kPa of partial steam pressure and 500°C for 9 h.

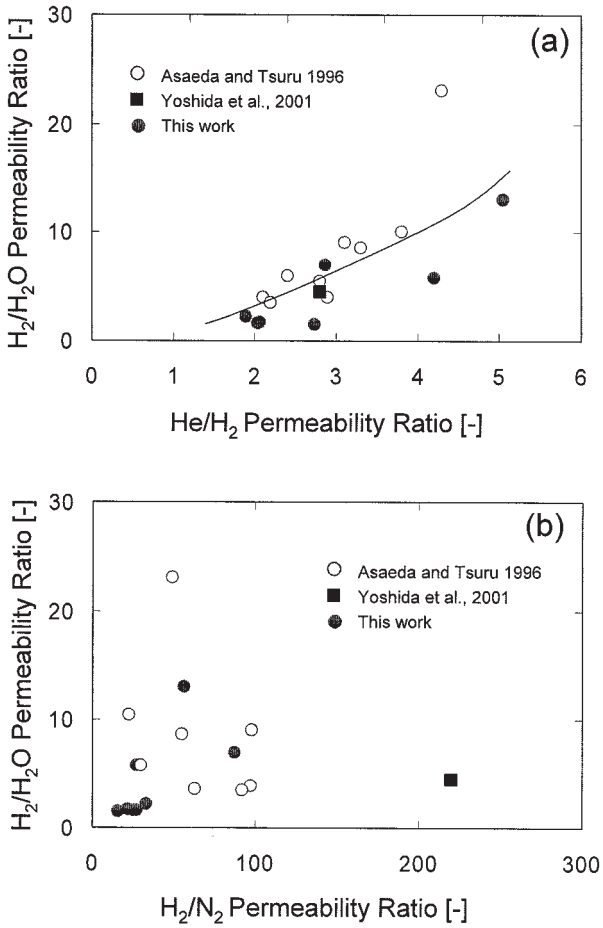

Figure 10. $\alpha(H_2/H_2O)$ as a function of $\alpha(He/H_2)$ (a) and $\alpha(H_2/N_2)$ (b) for microporous silica membranes prepared by a sol–gel process.

As indicated in reports of our previous studies (Tsuru et al. 2001; Yoshida et al. 2001b,c), steam, at a high temperature, affects the permeation performance of porous silica membranes prepared by a sol–gel process. Figure 9 shows the permeances of pure He, H_2, and N_2 before and after the hydrothermal treatment, the condition of which was a partial pressure of steam of 50 kPa in the feed at 500°C for 9 h. Permeances for hydrogen and helium deceased after the hydrothermal treatment, whereas that for nitrogen remained essentially unchanged. The effect of hydrothermal treatment can be interpreted as follows: the hydrothermal treatment densified the small pores through which H_2 and He were able to permeate and molecules of larger size could not, and the large pores that allowed permeation of large molecules, possibly corresponding to pinholes in the hydrogen separation layer, were unaffected by the treatment (Tsuru et al., 2001; Yoshida et al., 2001b).

Figure 10a and b shows the permeability ratios of hydrogen over steam, $\alpha(H_2/H_2O)$, as a function of those of helium over hydrogen $\alpha(He/H_2)$ and hydrogen over nitrogen $\alpha(H_2/N_2)$ for 16 microporous silica membranes prepared by the sol–gel method. $\alpha(H_2/H_2O)$, ranging from 1 to 20, showed a relatively good correlation with $\alpha(He/H_2)$, ranging from 1 to 5, although the correlation of $\alpha(H_2/H_2O)$ with $\alpha(H_2/N_2)$ was found to be scattered. This is probably because He (kinetic diameter 0.27 nm), H_2 (0.289), and H_2O (0.265), which have small kinetic diameters, permeated through similar pores: micropores formed as silica network structures (intraparticle pores) as well as large pores (interparticle pores) such as pinholes, whereas nitrogen permeates only through relatively large interparticle pores. Membrane performances used for catalytic membrane reaction are summarized in Table 4.

Membrane reaction of methane reforming

Figure 11 shows the time course for the conversion and flow rate during steam reforming (SRM) and oxygen-added steam reforming (OSR) reactions with/without membrane permeation. For the case of SRM, the conversion of methane without membrane permeation, which was achieved by closing the permeate stream, showed approximately the same value as the equilibrium conversion of 0.44 at 100 kPa, and increased with membrane permeation where the permeate stream was evacu-

Table 4. Membrane Performance Used for Experiments of Catalytic Membrane Reaction

Membrane	P_{H_2}* [mol m^{-2} s^{-1} Pa^{-1}]	$\alpha(H_2/N_2)$* [—]	$\alpha(H_2/H_2O)$ [—]
M-1	2.6×10^{-7} (2.0×10^{-7})	87 (69)	8
M-2	5.6×10^{-8} (5.1×10^{-8})	56 (48)	10
M-3	4.5×10^{-8}	42	8

*Values in parentheses indicate permeance and selectivity after catalytic reactions.

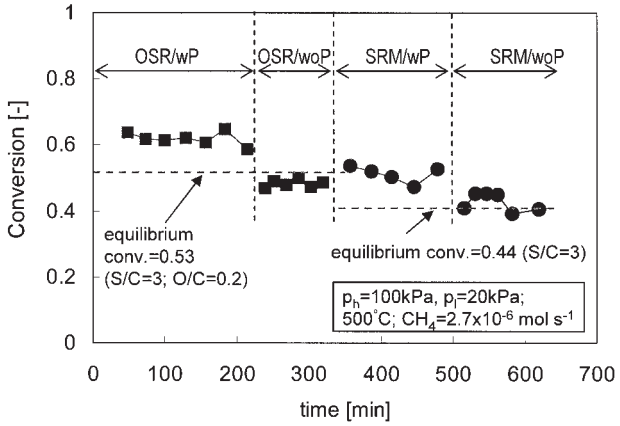

Figure 11. Time course for the conversion for a methane reforming reaction with and without membrane permeation.

SRM: steam reforming (S/C = 3); OSR: SRM with addition of oxygen (S/C = 3, O/C = 0.2); with and without membrane permeation (wP and woP).

ated to approximately 20 kPa. For the case of OSR with an oxygen addition of O/C = 0.2, the value for methane conversion without membrane permeation was larger than that of SRM because of methane combustion, and increased with membrane permeation.

Figure 12 shows a temperature profile along the axis; the temperature of the outside of the membrane housing was maintained at 500°C and the temperature inside the cylindrical membrane was measured by moving the location of the thermocouple inside the membrane. The temperature along the membrane axis was 500 ± 5°C under conditions of N_2 flow. For the case of the SRM reaction without membrane permeation, the inside temperature, which was 490°C at the inlet because of the endothermic reaction, increased along the axial direction and approached the same temperature profile as that for nitrogen flow, indicating that SRM occurred mainly in the first half of the membrane and no reaction occurred in the last half. With membrane permeation, the temperature decreased several degrees Celsius; this effect was clearly observed for the last half of the membrane length. This indicates that the endothermic SRM reaction of Eqs. 1–3 was enhanced by membrane permeation. For the case of OSR, the temperature was approximately 510°C at the inlet, decreased drastically, and then had approximately the same profile as that for N_2 flow, especially in the last half of the catalytic membrane. No oxygen was detected in the permeate or retentate stream, suggesting that the exothermic reaction of methane combustion occurred near the inlet, followed by an endothermic steam reforming reaction. With membrane permeation, the temperature profile decreased by several degrees Celsius, similar to SRM. Based on the temperature profile, it would be expected that the reaction of methane reforming could be autothermal, if the controlled addition of oxygen along the catalytic membrane is possible.

Figure 13 shows data on the conversion of methane (X_{CH4}), hydrogen yield (Y_{H2}), and flow rate of the retentate and permeate streams, which was defined as a total flow rate from the membrane reactor maintained at 500°C, when a microporous silica membrane, M-1, was used. Conversion without membrane permeation showed an approximately equilibrium conversion, indicating that the reaction rate was sufficiently high to assume an infinite Da number in the experimental ranges of methane feed flow rate. X_{CH4}, which was increased with membrane permeation, and hydrogen yield Y_{H2} increased to approximately 0.8 and 3, respectively, with a decrease in CH_4 feed flow rate. Figure 14 demonstrates the case where a microporous silica membrane, M-2, was used. These data show a tendency similar to that shown in Figure 13. It should be noted that hydrogen mole fraction of 0.95–0.98 (dry-gas basis) was achieved in permeate stream for both experimental conditions. However, because M-2 had a relatively low hydrogen permeance of 5.6×10^{-8} mol m^{-2} s^{-1} Pa^{-1}, the flow rate of permeate and retentate crossed at a relatively low F_{CH_4} of 1×10^{-6} mol s^{-1}, whereas M-1 showed a cross at F_{CH_4} of 5×10^{-6} mol s^{-1}. The curves in the figures were calculated using the isothermal plug-flow model, as described earlier, assuming infinite Da. Membrane parameters measured by single gases before and after reaction, and used for calculation, are summarized in Table 4. Because the permeance change of M-1 before and after the reaction was relatively large, two calculated curves are shown in Figure 13. In both figures calculated curves for conversion, hydrogen yield, and flow rates are in a relatively good agreement with experimental data, although the comparison of simulated curves with experimental data is not

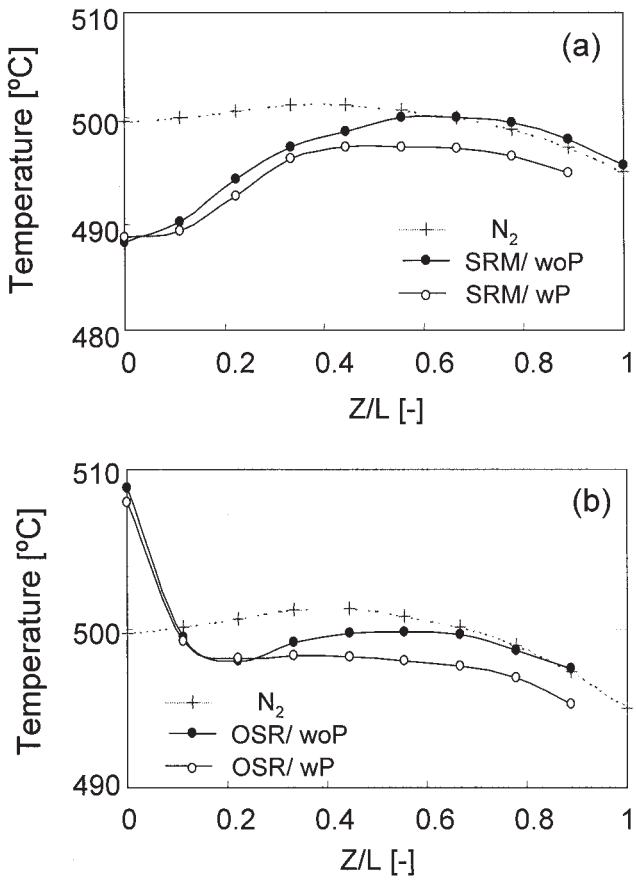

Figure 12. Temperature profile along the axial direction for SRM (a) and OSR (b).

$F_{CH_4} = 1.3 \times 10^{-5}$ mol s^{-1}; S/C = 3, O/C = 0.2; p_h = 100 kPa, p_l = 20 kPa.

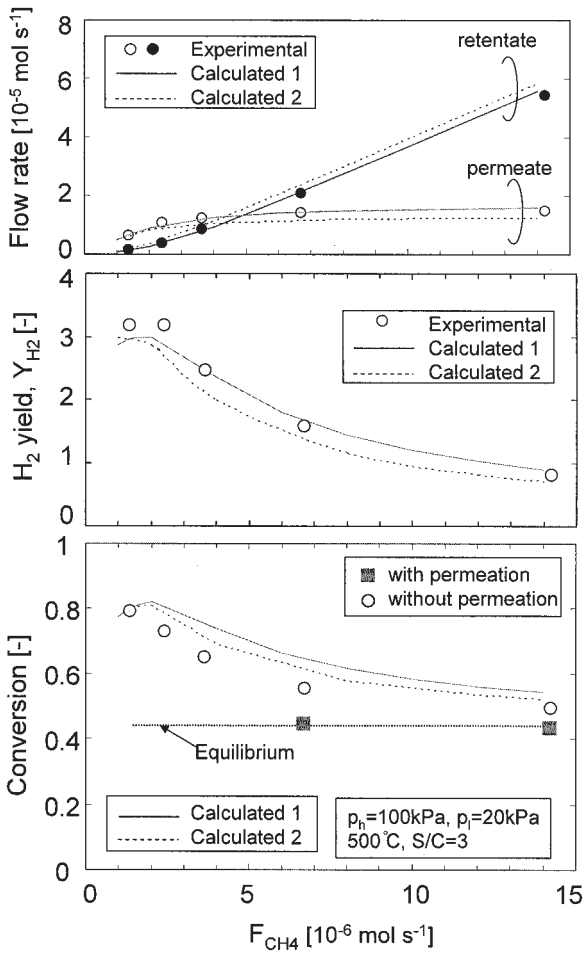

Figure 13. Flow rate in the permeate and retentate, hydrogen yield, and CH_4 conversion as a function of CH_4 inlet flow rate.

M-1; SRM; p_h = 100 kPa, p_l = 20 kPa; S/C = 3; P_{H_2} = $2.6 \times 10^{-7}/2.0 \times 10^{-7}$ mol m^{-2} s^{-1} Pa^{-1}, $\alpha(H_2/N_2)$ = 87/69 before/after reaction; $\alpha(H_2/H_2O)$ = 8; calculations 1 and 2 were simulated using permeances before and after reaction.

based on the exact model in terms of catalyst configuration and temperature profile. M-1 was not in as good agreement as M-2, probably because a larger permeance might cause a concentration gradient in the radial direction inside the catalyst layer inside a support, a factor that was not considered in the present simple simulation model.

Figure 15 shows the effect of permeate pressure on catalytic membrane performance under conditions of constant feed side pressure and constant feed flow rate. With a decrease in permeate pressure, methane conversion and hydrogen yield were increased. This can be explained by an increased driving force for the permeation of hydrogen, as evidenced by the permeate flow rate. Again, the calculated curves are in relatively good agreement with experimental data.

Conclusions

Methane steam reforming, with and without oxygen addition, was theoretically and experimentally investigated using microporous silica membranes, which allow the permeation of hydrogen as well as the feed and reactant gases based on permselectivity. A simulation of catalytic membrane reactors was carried out in a cocurrent, isothermal, plug-flow–type membrane reactor with the selective permeation of hydrogen through microporous membranes. The effect of operating conditions on the conversion of methane and the production of hydrogen was discussed using two dimensionless numbers, the Damköhler number and the permeation number θ. Methane conversion, X_{CH4}, shows approximately the same dependency on permeation number in terms of permeability ratios of hydrogen over nitrogen, whereas hydrogen purity in the permeate decreased with an increase in hydrogen selectivity. The dimensionless numbers, permeation number θ and Damköhler number Da, are quite useful parameters in understanding the dependency of the performance of a membrane reactor on operating conditions (feed flow rate, reaction rate determined by types of catalyst, and the amount of catalyst in the membrane reactor) and membrane performance (hydrogen permeance, permeability ratio to other gases) for methane reforming reaction.

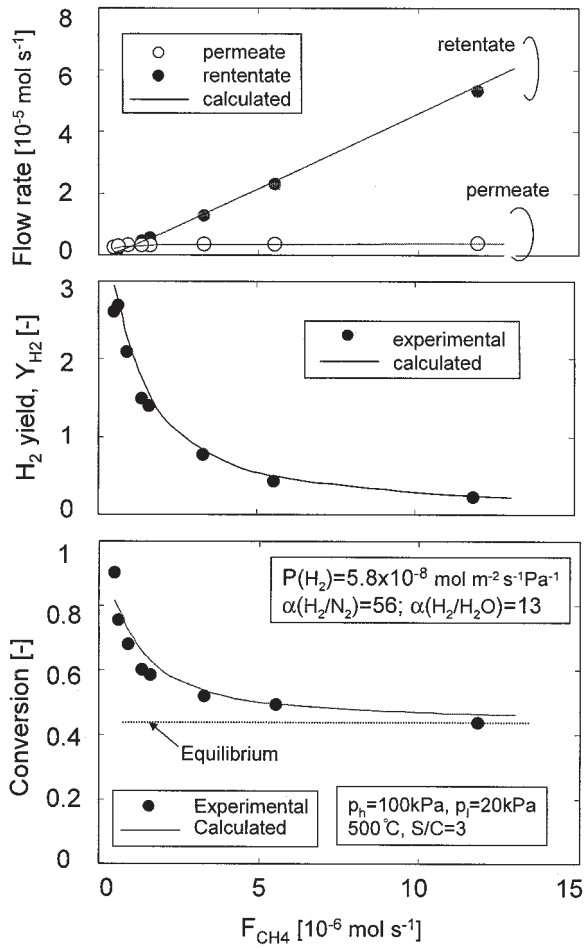

Figure 14. Flow rate in permeate and retentate, hydrogen yield, and CH_4 conversion as a function of CH_4 inlet flow rate.

M-2; SRM; p_h = 100 kPa, p_l = 20 kPa; S/C = 3; P_{H_2} = $5.6 \times 10^{-8}/5.1 \times 10^{-8}$, $\alpha(H_2/N_2)$ = 56/48, before/after reaction; $\alpha(H_2/H_2O)$ = 10; curves are calculated.

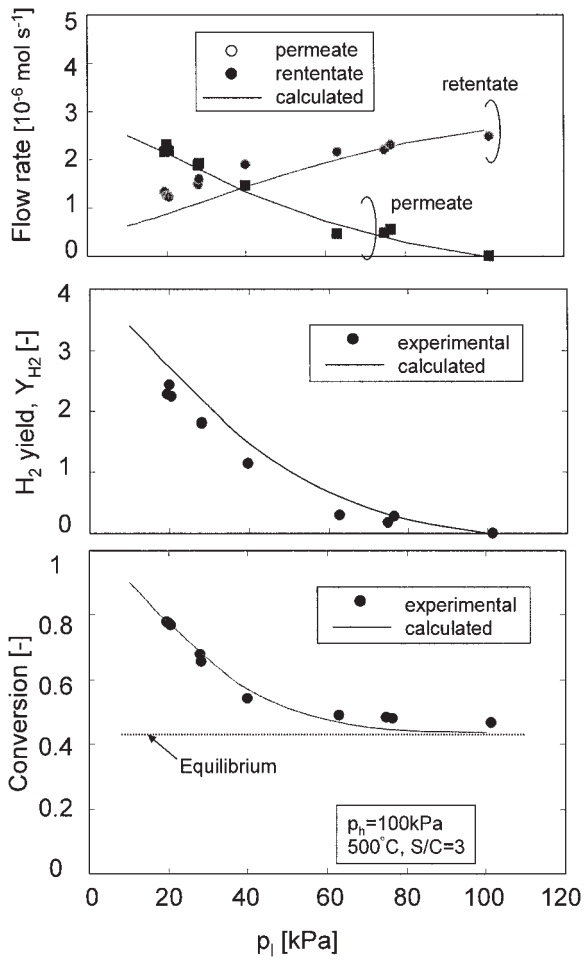

Figure 15. Flow rate in the permeate and retentate, hydrogen yield, and CH_4 conversion as a function of permeate pressure.

M-3; SRM; p_h = 100 kPa; $F_{CH_4} = 4.5 \times 10^{-6}$ mol s^{-1}; S/C = 3; $P_{H_2} = 4.5 \times 10^{-8}$, $\alpha(H_2/N_2) = 42$, $\alpha(H_2/H_2O) = 8$; curves are calculated.

Catalytic membrane reactors, consisting of a silica microporous layer and a Ni-catalyst layer, were prepared. The permeability ratio of hydrogen over steam, $\alpha(H_2/H_2O)$, which ranged from 1 to 20, showed a relatively good correlation with that for helium over hydrogen, $\alpha(He/H_2)$, suggesting He, H_2, and H_2O permeated through similar pores such as micropores and large pores. Catalytic membrane reactors showing hydrogen selectivity over nitrogen of 30–100, with a hydrogen permeance of 0.5–3 $\times 10^{-7}$ mol m^{-2} s^{-1} Pa^{-1}, were applied to the steam reforming of methane. The reaction was carried out at 500°C, and the feed and permeate pressures were maintained at 100 and 20 kPa, respectively. Methane conversion X_{CH4} increased to approximately 0.8 beyond the equilibrium conversion of 0.44 by extracting hydrogen in the permeate stream, and the permeated hydrogen yield Y_{H2} reached a maximum of 3 with membrane permeation. The experimental results were found to be in reasonably good agreement with the simulations.

Acknowledgment

This work was supported by the R&D Project for High Efficiency Hydrogen Production/Separation System using Ceramic Membranes Funded by NEDO, Japan.

Notation

Da = Damköhler number, Da = $R_1^{max} W_{cat}/F_{CH_4,0}$
F_i = feed-side molar flow rate of species i, mol s^{-1}
$F_{i,0}$ = feed molar flow rate of species i, mol s^{-1}
$F_{i,L}$ = outlet feed-side molar flow rate of species i, mol s^{-1}
f_i = dimensionless flow rate of species i, $F_i/F_{CH_4,0}$
K_i = adsorption parameters, as defined in Table 1
K_{je} = equilibrium constant, as defined in Table 1
k_i = rate factors, as defined in Table 1
L = reactor length, m
P_i = permeance of species i, mol s^{-1} m^{-2} Pa^{-1}
p_h = feed-side pressure, Pa
p_i = partial pressure of species i, Pa
p_l = permeate-side pressure, Pa
p_r = pressure ratio, p_l/p_h
Q_i = permeate-side molar flow rate of species i, mol s^{-1}
$Q_{i,L}$ = outlet permeate-side molar flow rate of species i, mol s^{-1}
q_i = dimensionless flow rate of species i, $Q_i/F_{CH_4,0}$
R_j = reaction rate, mol kg-cat^{-1} s^{-1}
R_j^* = dimensionless reaction rate, R_j/R_1^{max}
R_1^{max} = maximum forward reaction rate of Eq. 1, $R_1^{max} = k_1(p_{CH_4}p_{H_2O}/p_{H_2}^{2.5})/DEN^2$, mol kg-$cat^{-1}$ s^{-1}
s = membrane area per unit membrane length, m^2 m^{-1}
w_{cat} = catalyst weight per unit membrane axial length, kg-cat m^{-1}
W_{cat} = catalyst weight of membrane module ($W_{cat} = w_{cat}L$), kg-cat
X_{CH4} = methane conversion, $X_{CH_4} = 1 - (F_{CH_4,L} + Q_{CH_4,L})/F_{CH_4,0}$
x_i = feed-side mole fraction of species i
Y_{H2} = permeate hydrogen yield, the ratio of permeated hydrogen molar flow rate to feed methane flow rate, $Y_{H_2} = Q_{H_2,L}/F_{CH_4,0}$
y_i = permeate-side mole fraction of species i
z = axial coordinate, m

Greek letters

α_i = permeability ratio of hydrogen over species i, P_{H_2}/P_i
θ = permeation number, $\theta = P_{H_2} s L p_h / F_{CH_4,0}$
$\nu_{i,j}$ = stoichiometric coefficient of species i in reaction j
ς = dimensionless axial coordinate, z/L

Literature Cited

Adris, A. M., S. S. E. H. Elnashaie, and R. Hughes, "A Fluidized Bed Membrane Reactor for the Steam Reforming of Methane," *Can. J. Chem. Eng.*, **69**, 1061 (1991).

Asaeda, M., and T. Tsuru, "Development of Porous Ceramic Membranes for Hydrogen Separation at High Temperature," Reports on Principle of Exergy Reproduction, supported by the Grant-in-Aid on Priority Area, Minister of Education, Japan (1997).

Asaeda, M., and S. Yamasaki, "Separation of Inorganic/Organic Gas Mixtures by Porous Silica Membranes," *Sep. Pur. Technol.*, **25**, 151 (2001).

Chai, M., M. Machida, K. Eguchi, and H. Arai, "Promotion of Hydrogen Permeation on Metal-Dispersed Alumina Membranes and Its Application to a Membrane Reactor for Methane Steam Reforming," *Appl. Catal. A Gen.*, **110**, 239 (1994).

Chen, Z., Y. Yan, and S. S. E. H. Elnashaie, "Modeling and Optimization of a Novel Membrane Reformer for Higher Hydrocarbon," *AIChE J.*, **49**, 1250 (2003).

Grace, J. R., X. Li, and C. J. Lim, "Equilibrium Modeling of Catalytic Steam Reforming of Methane in Membrane Reactors with Oxygen Addition," *Catal. Today*, **64**, 141 (2001).

Hsieh, H. P., *Inorganic Membranes for Separation and Reaction*, Elsevier Science, Amsterdam (1996).

Hwang, G.-H., and K. Onuki, "Simulation Study on the Catalytic Decomposition of Hydrogen Iodide in a Membrane Reactor with a Silica Membrane for the Thermochemical Water-Splitting IS Process," *J. Membr. Sci.*, **194**, 207 (2001).

Ito, N., Y. Shindo, K. Haraya, K. Obata, T. Hakuta, and H. Yoshitome, "Simulation of a Reaction Process with a Membrane Separation," *Kagaku Kogaku Ronbunshu*, **9**, 572 (1983).
Kim, J. H., B. S. Choi, and J. Yi, "Modified Simulation of Methane Steam Reforming in Pd-Membrane/Packed-Bed Type Reactor," *J. Chem. Eng. Jpn.*, **32**, 760 (1999).
Kurugot, S., T. Yamaguchi, and S. Nakao, "Rh/Gamma-Al_2O_3 Catalytic Layer Integrated with Sol–Gel Synthesized Microporous Silica Membrane for Compact Membrane Reactor Applications," *Catal. Lett.*, **86**, 273 (2003).
Mohan, K., and R. Govind, "Analysis of a Cocurrent Membrane Reactor," *AIChE J.*, **32**, 2083 (1986).
Mohan, K., and R. Govind, "Analysis of Equilibrium Shift in Isothermal Reactors with a Permselective Wall," *AIChE J.*, **34**, 1493 (1988).
Oklany, J. S., K. Hou, and R. Hughes, "A Simulative Comparison of Dense and Microporous Membrane Rectors for the Steam Reforming of Methane," *Appl. Catal. A Gen.*, **170**, 13 (1998).
Prabhu, A. K., A. Liu, L. G. Lovell, and T. Oyama, "Modeling of the Methane Reforming Reaction in Hydrogen Selective Membrane Reactors," *J. Membr. Sci.*, **177**, 83 (2000b).
Prabhu, A. K., and T. Oyama, "Highly Hydrogen Selective Ceramic Membranes: Application to the Transformation of Greenhouse Gases," *J. Membr. Sci.*, **176**, 233 (2000a).
Sanches, J. G., and T. T. Tsotsis, *Catalytic Membranes and Membrane Reactors*, Wiley-VCH, New York (2002).
Sea, B. K., E. Soewito, M. Watanabe, K. Kusakabe, S. Morooka, and S. S. Kim, "Hydrogen Recovery from a H_2–H_2O–HBr Mixture Utilizing Silica-Based Membranes at Elevated Temperatures. 1. Preparation of H_2O- and H_2-Selective Membranes," *Ind. Eng. Res.*, **37**, 2502 (1998).
Tsotsis, T. T., A. M. Champaginie, S. P. Vasileiadis, Z. D. Ziaka, and R. G. Minet, "The Enhancement of Reaction Yield through the Use of High Temperature Membrane Reactor," *Sep. Sci. Technol.*, **28**, 397 (1993).
Tsuru, T., S. Izumi, T. Yoshioka, and M. Asaeda, "Effect of Temperature on Transport Performance of Neutral Solutes through Inorganic Nanofiltration Membranes," *AIChE J.*, **46**, 565 (2000).
Tsuru, T., H. Takezoe, and M. Asaeda, "Ion Separation by Porous Silica–Zirconia Nanofiltration Membranes," *AIChE J.*, **44**, 765 (1998).
Tsuru, T., T. Tsuge, S. Kubota, K. Yoshida, T. Yoshioka, and M. Asaeda, "Catalytic Membrane Reaction for Methane Steam Reforming Using Porous Silica Membranes," *Sep. Sci. Technol.*, **36**, 3721 (2001).
Uemiya, S., N. Sato, H. Ando, T. Matsuda, and E. Kikuchi, "Steam Reforming of Methane in a Hydrogen-Permeable Membrane Reactor," *Appl. Catal.*, **67**, 223 (1991).
Xu, J., and G. F. Froment, "Methane Steam Reforming, Methananation and Water-Gas Shift. 1. Kinetics," *AIChE J.*, **35**, 88 (1989).
Yogeshwar, V., V. Gokhale, R. D. Noble, and J. F. Falconer, "Effect of Reactant Loss and Membrane Selectivity on a Dehydrogenation Reaction in a Membrane-Enclosed Catalytic Reactor," *J. Membr. Sci.*, **103**, 235 (1995).
Yoshida, K., Y. Hirano, H. Fujii, T. Tsuru, and M. Asaeda, "An Application of Silica–Zirconia Membrane for Hydrogen Separation to Membrane Reactor," *Kagaku Kogaku Ronbunshu*, **27**, 657 (2001a).
Yoshida, K., Y. Hirano, H. Fujii, T. Tsuru, and M. Asaeda. "Development of Silica–Zirconia Membrane for Hydrogen Separation at High Temperature and Effect of Zirconia Content on Hydrogen Permeation," *Kagaku Kogaku Ronbunshu*, **27**, 106 (2001b).
Yoshida, K., Y. Hirano, H. Fujii, T. Tsuru, and M. Asaeda, "Hydrothermal Stability and Performance of Silica–Zirconia Membranes for Hydrogen Separation in Hydrothermal Conditions," *J. Chem. Eng. Jpn.*, **27**, 657 (2001c).
Yoshioka, T., E. Nakanishi, T. Tsuru, and M. Asaeda, "Experimental Study of Gas Permeation through Microporous Silica Membranes," *AIChE J.*, **47**, 2052 (2001).

Manuscript received Aug. 22, 2003, and revision received Feb. 19, 2004.